

Linear magnetic flux amplifier

D. S. Golubović and V. V. Moshchalkov

INPAC - Institute for Nanoscale Physics and Chemistry,

Nanoscale Superconductivity and Magnetism Group,

Laboratory for Solid State Physics and Magnetism,

K. U. Leuven, Celestijnenlaan 200 D, B-3001 Leuven, Belgium

By measuring the critical current versus the applied magnetic field $I_c(\Phi)$ of an Al superconducting loop enclosing a soft Permalloy magnetic dot, we demonstrate that it is feasible to design a linear magnetic flux amplifier for applications in superconducting quantum interference devices. The selected dimensions of a single-domain Permalloy dot provide that the preferential orientation of the magnetization is rotated from the perpendicular direction. By increasing an applied magnetic field, the magnetization of the dot coherently rotates towards the out-of-plane direction, thus providing a flux gain and an enhancement of the sensitivity. As a result of a pronounced shape anisotropy, the flux gain generated by the dot can be tuned by adjusting the dimensions of the dot.

PACS numbers: 74.78.Na., 75.75.+a, 74.25.Dw

The Superconducting Quantum Interference Device (SQUID) is the most sensitive magnetic field sensor that has been widely used for various applications - from the nuclear magnetic resonance in medicine to quantum computing [1, 2]. As the voltage - flux $V(\Phi)$ characteristic of SQUIDs is highly nonlinear, they are commonly used in the flux-locked loop, where a magnetically coupled feedback provides that the SQUID operates around the steepest part of the $V(\Phi)$ characteristic [1, 3]. A lot of effort is focused on enhancing the sensitivity and minimizing the noise in SQUID systems (see [3] and references therein). Recently, $\pi/2$ - and π -SQUIDs based on d-wave superconductors have been investigated as the possible candidates for SQUIDs without the external flux bias [4, 5, 6]. Soft ferromagnetic materials have been used as another means to improve the sensitivity of SQUID magnetometers [7, 8, 9]. Even though soft ferromagnets provide an enhancement of sensitivity, they are generally considered unfavorable because magnetization switching, domain wall nucleation and motion, as well as additionally generated vortices can substantially increase the noise.

Sub-micrometre magnetic elements are in the single-domain state and the magnetization reversal occurs through the coherent rotation [10, 11]. By using Landau-Lifshitz-Gilbert equation the settling time of a sub-micrometre soft magnetic element in the single domain state is found to be less than 10 ns, which means that such an element does not distort the applied magnetic field in its vicinity, nor is the magnetization rotation retarded up to the GHz frequency range [12].

We propose to use a soft sub-micrometre magnetic dot as a flux amplifier for SQUID applications. If the height of a soft dot is slightly smaller than its diameter, the magnetization is oriented neither in-plane nor out-of-plane, as shown in Fig. 1(a) [11]. By applying a perpendicular magnetic field, the out-of-plane component of the magnetization increases and, accordingly, the total flux generated by the dot along the out-of-plane direction increases, as shown in Fig. 1(b). If such a dot is placed at the centre of the pick-up loop of a SQUID, it can act as a built-in flux amplifier.

The properties of the flux amplifier have been studied by measuring the critical current versus the applied magnetic field $I_c(\Phi)$ of a superconducting loop with a soft magnetic dot at its centre. The samples were prepared using electron beam lithography and lift-off procedure in two steps. In the first step 45 nm thick Al loops were prepared by thermal evaporation, whereas in the second step 90 nm thick polycrystalline $Ni_{0.8}Fe_{0.2}$ Permalloy (Py) dots were grown by electron beam evaporation. Two samples hereafter referred to as

the 'Sample A' and 'Sample B', as well as a reference Al loop without a Py dot have been measured. Fig. 2 shows a scanning electron micrograph of the Sample B. The white bar corresponds to $1\ \mu\text{m}$. The hysteresis loop of an array of the co-evaporated reference Py dots measured at 5 K in the perpendicular magnetic field is shown in Fig. 3. The inset in Fig. 3 shows that the magnetization of the dots depends linearly on the applied field in the range $|\mu_0 H_a| \leq 15\ \text{mT}$. The inner and the outer radii of the Sample A are $r_{iA} = 0.73\ \mu\text{m}$ and $r_{oA} = 0.94\ \mu\text{m}$, the radius of the Py dot is $r_{dA} = 0.12\ \mu\text{m}$, whereas for the sample B $r_{iB} = 0.73\ \mu\text{m}$, $r_{oB} = 0.92\ \mu\text{m}$ and $r_{dB} = 0.115\ \mu\text{m}$. The radii of the reference sample are $r_{iR} = 0.73\ \mu\text{m}$ and $r_{oR} = 0.95\ \mu\text{m}$, respectively. The critical temperatures of the Samples A and B are $T_{c0A} = 1.4571\ \text{K}$ and $T_{c0B} = 1.4557\ \text{K}$, whereas the critical temperature of the reference sample is $T_{c0R} = 1.4591\ \text{K}$. The superconducting coherence length is $\xi(0) = 117\ \text{nm}$ and the penetration depth is $\lambda(0) = 374\ \text{nm}$ or $\kappa \approx 3.2$. Since at the temperatures close to the zero-field critical temperature T_{c0} the superconducting coherence length $\xi(T)$ is greater than the radius of the loop, the presence of the non-current-carrying voltage contacts creates two parallel weak links and the $I_c(\Phi)$ of the loop has the same periodicity as the $I_c(\Phi)$ of the SQUID [13].

The measurements have been carried out in the DC mode, with the current and field steps of $10\ \text{nA}$ and $50\ \mu\text{T}$, respectively. The field and transport current were set in the order which ensures that no flux can be trapped in the samples over the course of the measurements.

The upper part of Fig. 4 shows the $I_c(\Phi)$ -curves of the Sample A taken at $0.997T_{c0A}$, $0.995T_{c0A}$ and $0.993T_{c0A}$, whereas the lower part shows the $I_c(\Phi)$ -curves of the Sample B at $0.995T_{c0B}$, $0.994T_{c0B}$ and $0.992T_{c0B}$. A higher critical current corresponds to a lower temperature. The critical currents were determined using the conventional $1\ \mu\text{V}$ -criterion.

Open symbols in Fig. 4 are the experimental data, whereas the solid lines are the theoretical curves, obtained using the expression for the critical current of an asymmetric SQUID, modified to take into account the influence of the soft dots [6]

$$I_c(\Phi) = \left(A + B \cos \left[2\pi \left(\frac{\Phi}{\Phi_0} + g_m \frac{\Phi}{\Phi_0} \right) \right] \right)^{1/2} \quad (1)$$

whereby A and B are constants with the dimension $[A^2]$, Φ is the applied flux, Φ_0 is the superconducting flux quantum and g_m is the gain provided by the magnetic dot. Given the linear dependence of the magnetization on the applied magnetic field (see Fig. 3), the flux gain provided by the dots has been taken constant. The flux Φ has been calculated with

respect to the means radius $r_m = (r_o + r_i)/2$, as at the lowest temperature measured of $0.992T_{c0B}$ the following condition is valid $\xi(T) \gg r_o - r_i$ ($(\xi(0.992T_{c0B}) \approx 1.3 \mu\text{m}, r_{oB} - r_{iB} = 0.187 \mu\text{m})$). The 1D-character of the order parameter in the loops is of an extreme importance for the validity of the measurements, because it ensures that the radius over which the fluxoid quantization occurs does not change with the temperature and/or field, thus ruling out any inherent change in the periodicity of the $I_c(\Phi)$ -curves [14]. The constants A and B have been chosen so as to provide the best amplitude agreement, whereas for both samples, irrespective of the temperature, the gain provided by the dot is $g_m = 0.1$, which means that for this particular dimensions the Py dot provides a 10 % enhancement of the sensitivity. For comparison, Fig. 5 shows the $I_c(\Phi)$ -curve of the reference sample taken at $0.994T_{c0R}$. Filled symbols are the experimental data, whereas the solid line is the theoretical curve obtained by setting $g_m = 0$ in Eq. (1). It is clear that without a Py dot, the $I_c(\Phi)$ -curve has the periodicity Φ_0 , independent of an applied magnetic field.

A moderate gain of only 10 % is caused by the low thickness (only 150 nm) of the electron beam resist, which limited the maximum achievable height of Py dots and, in turn, constrained the radius of the dot. An increase and adjustment of the gain can be accomplished by using thicker resists, which would allow to increase the height and radius of a Py dot, whilst keeping the height/diameter ratio which provides a rotated preferential direction of the magnetization.

Fig. 6 shows the voltage-current (IV) curves of the Sample B at $1.85\Phi_0$ and $2\Phi_0$ (open symbols), and $2.75\Phi_0$ and $3\Phi_0$ (filled symbols) taken at $0.994T_{c0B}$. The horizontal lines indicate the voltage criterion used. Non-integer values of the flux in Fig. 6 correspond to the maxima in $I_c(\Phi)$ -curves shown in Fig. 4. The IV-curves explicitly show that as the applied magnetic field increases, the difference between the flux values whereat a maximum in the critical current appears and the closest integer flux ($n\Phi_0, n \in \mathbf{Z}$) increases. We note that neither local heating nor non-equilibrium effects have been observed in the IV-curves [15]. This clearly implies that the contraction of the period of the $I_c(\Phi)$ -curves comes from the magnetic dot.

In conclusion, we have fabricated and investigated a magnetic flux amplifier for SQUID applications. By measuring $I_c(\Phi)$ -curves it has been demonstrated that a Py magnetic dot provides a linear flux amplification. The design proposed makes it possible to tune the flux gain by adjusting the height/diameter ratio of a Py dot.

This work has been supported by the Research Fund K. U. Leuven GOA/2004/02 programme, the Flemish FWO and the Belgian IUAP programmes, as well as by the JSPS/ESF "Nanoscience and Engineering in Superconductivity" programme.

- [1] J. R. Kirtley, M. B. Ketchen, C. C. Tsuei, J. Z. Sun, W. J. Gallagher, L. S. Yu-Jahnes, A. Gupta, K. G. Stawiasz and S. J. Wind, *IBM J. Res. Develop.* **39**, 655 (1995).
- [2] I. Chiorescu, Y. Nakamura, C. J. P. M. Harmans and J. E. Mooij, *Science* **299**, 1869 (2003).
- [3] D. Drung, *Supercond. Sci. Technol.* **16**, 1320 (2003).
- [4] M. H. S. Amin, M. Coury and G. Rose, *IEEE Trans. Appl. Superconduct.* **12** (2002).
- [5] B. Chesca, R. R. Schultz, C. W. Schneider, H. Hilgenkamp and J. Mannhart, *Phys. Phys. Lett.* **88**, 177003 (2002).
- [6] H. J. H. Smilde, Ariando, D. H. A. Blank, H. Hilgenkamp and H. Rogalla, *Phys. Rev. B* **70**, 024519 (2004).
- [7] U Poppe, M. I. Faley, E. Zimmermann, W. Glaas, I Breunig, R Speen, B. Jungbluth, H. Soltner, H Halling and K Urban, *Supercond. Sci. Technol.* **17**, S191 (2004).
- [8] B Baek, S. H. Moon, S. Y. Lee, S. M. Lee, J. I. Kye, H. J. Lee and Z. G. Kim, *Supercond. Sci. Technol.* **17**, 1022 (2004).
- [9] K. Tanaka, T. Morooka, A. Odawara, K. Chinone, Y. Mawatary and M. Koyanagi, *Apply. Phys. Lett* **77**, 1677 (2000).
- [10] W. Rave and A. Hubert, *IEEE Trans. Magn.* **36**, 3886 (2000).
- [11] R. P. Cowburn, *J. Phys. D: Appl. Phys* **33**, R1 (2000).
- [12] G. Albuquerque, J. Miltat and A. Thiaville, *J. Appl. Phys.* **89**, 6719 (2001).
- [13] V. V. Moshchalkov, L. Gielen, M. Dhalle, C. Van Haesendonck and Y. Bruynseraede, *Nature* **361**, 617 (1993).
- [14] D. Y. Vodolazov, B. J. Baelus and F. M. Peeters, *Phys. Rev. B* **66**, 054531 (2002).
- [15] A. Brinkman, A. A. Golubov, H. Rogalla, F. K. Wilhelm and M. Y. Kupriyanov, *Phys. Rev. B* **68**, 224513 (2003).

Figure Captions

Fig. 1 A schematic of the interaction of a soft magnetic dot with an applied magnetic flux.

Fig. 2 A scanning electron micrograph of an Al loop with a Py dot at the centre (Sample B). The white bar corresponds to $1 \mu\text{m}$.

Fig. 3 The hysteresis loop of Py dots used in the experiment measured at 5 K in the perpendicular field. The inset shows the magnetization of the dots for the applied fields $|\mu_0 H_a| \leq 15 \text{ mT}$.

Fig. 4 The $I_c(\Phi)$ -curves of the Sample A (upper part) taken at $0.997T_{c0A}$, $0.995T_{c0A}$ and $0.993T_{c0A}$ and Sample B (lower part) taken at $0.995T_{c0B}$, $0.994T_{c0B}$ and $0.992T_{c0B}$. Open symbols are the experimental data, whereas the solid lines are the theoretical curves. A higher critical current corresponds to a lower temperature.

Fig. 5 The $I_c(\Phi)$ -curve of the reference sample taken at $0.994T_{c0R}$. The filled symbols are the experimental data, whereas the solid line is the theoretical curve.

Fig. 6 The IV -curves of the Sample B at $0.994T_{c0B}$ for $\Phi = 1.85\Phi_0$, $\Phi = 2\Phi_0$, $\Phi = 2.75\Phi_0$ and $\Phi = 3\Phi_0$.

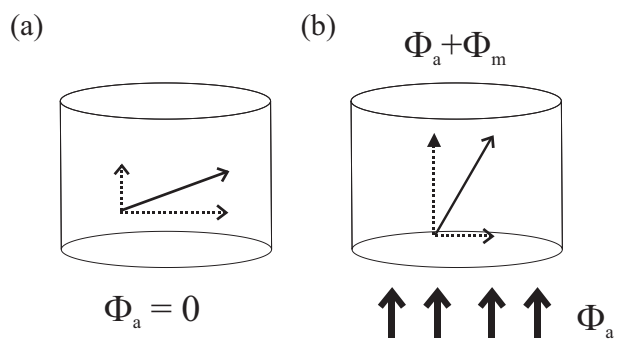


FIG. 1: D. S. Golubović and V. V. Moshchalkov

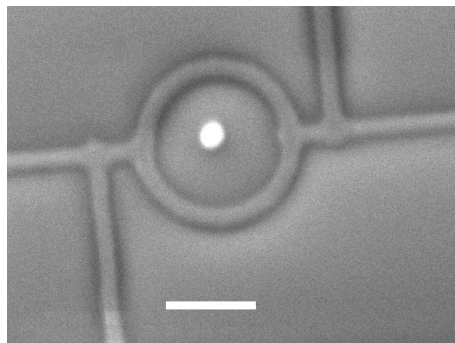


FIG. 2: D. S. Golubović and V. V. Moshchalkov

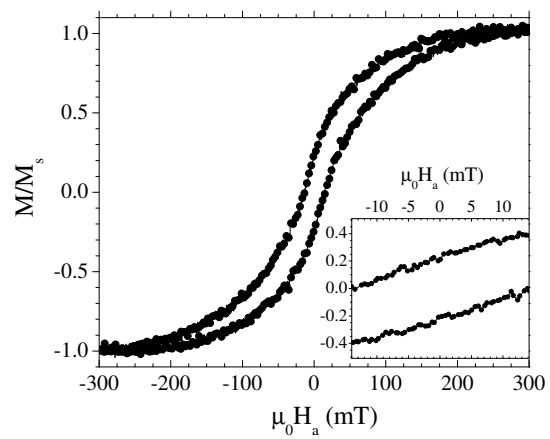


FIG. 3: D. S. Golubović and V. V. Moshchalkov

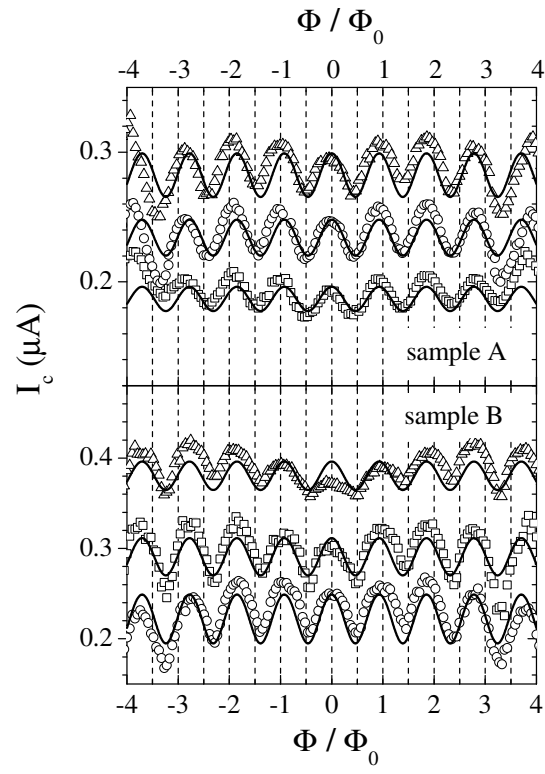


FIG. 4: D. S. Golubović and V. V. Moshchalkov

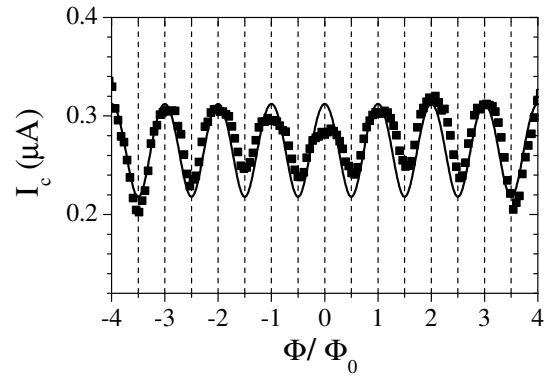


FIG. 5: D. S. Golubović and V. V. Moshchalkov

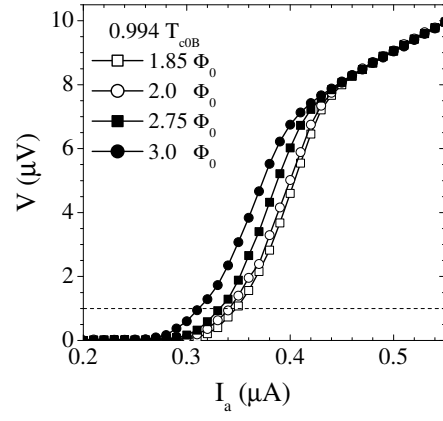


FIG. 6: D. S. Golubović and V. V. Moshchalkov